macromol

MDPI

Article

Ochratoxin A-Imprinted nanoMIPs Prepared by Solid Phase Synthesis: Effect of Mimic Template on Binding Properties

Thea Serra, Laura Anfossi, Simone Cavalera, Matteo Chiarello, Fabio Di Nardo, Valentina Testa and Claudio Baggiani *

Department of Chemistry, University of Torino, Via P. Giuria 7, 10125 Torino, Italy; thea.serra@unito.it (T.S.); laura.anfossi@unito.it (L.A.); simone.cavalera@unito.it (S.C.); matteo.chiarello@unito.it (M.C.); fabio.dinardo@unito.it (F.D.N.); v.testa@unito.it (V.T.)

* Correspondence: claudio.baggiani@unito.it

Abstract: The solid-phase polymerization synthesis (SPPS) represents one of the most innovative approaches to the preparation of nano-sized molecularly imprinted polymers. One of its main features consists of the use of a solid support on which the template molecule is covalently grafted. It implies that the imprinting process does not involve the target molecule as is, but, rather, a structural modification of it. It is known that the rationally designed mimic N-(4-chloro-1-hydroxy-2-naphthoylamido)-(L)-phenylalanine (CHNA-Phe) is able to generate, by bulk polymerization, imprinted materials capable of recognizing the mycotoxin Ochratoxin A (OTA). In this work, we wanted to verify whether the CHNA-Phe can be a useful mimic template in the SPPS technique. The binding isotherm were measured in the pH range of 4–8 and the binding affinities for CHNA-Phe and OTA were compared, showing that CHNA-Phe-imprinted nanoMIPs recognize, in buffered water, equally well OTA, and that the overall molecular recognition depends markedly from pH-related ionic interactions between the ligand and the binding site. There results confirm that in the SPPS method, it is possible and convenient to use as mimic templates a molecule whose three-dimensional structure is to some extent different from the target without substantial loss of selectivity or binding affinity.

Keywords: molecular imprinting; nanoMIP; solid-phase polymerization synthesis; mimic template; Ochratoxin A

Citation: Serra, T.; Anfossi, L.; Cavalera, S.; Chiarello, M.; Nardo, F.D.; Testa, V.; Baggiani, C. Ochratoxin A-Imprinted nanoMIPs Prepared by Solid Phase Synthesis: Effect of Mimic Template on Binding Properties. *Macromol* **2023**, *3*, 234–244. https://doi.org/10.3390/macromol3020015

Academic Editor: Ivan Gitsov

Received: 21 March 2023
Revised: 3 May 2023
Accepted: 10 May 2023
Published: 11 May 2023

1. Introduction

In recent years, the focus on molecularly imprinted polymers (MIPs) has progressively shifted from bulk materials characterized by micrometer-size dimensions and morphologies to materials of much smaller dimensions. Imprinted nanoparticles, or "nanoMIPs", present several practical advantages, including solubility in buffers and organic solvents, limited binding heterogeneity, reduced non-specific binding, and improved mass transfer and binding kinetics due to larger surface/mass ratio [1]. The solid-phase polymerization synthesis (SPPS)—illustrated in Scheme 1—represents one of the most innovative approaches to the preparation of nano-sized molecularly imprinted polymers (nanoMIPs). This method uses solid support glass beads covalently grafted with template molecules as a support for the polymerization process taking place in the interstitial space between the non-porous beads. The growth of lightly cross-linked polymeric chains near the glass surface results in the imprinting of the nascent nanoparticles onto the grafted template molecules, producing high affinity nanoMIPs [2]. Because of the strength of non-covalent interactions between nanoparticles and template molecules, at the end of the polymerization process, any residual monomers, polymerization by-products, and low affinity polymers can be easily removed by gentle washing, while high affinity nanoMIPs can be recovered later by washing with a solution capable of breaking the non-covalent molecular interactions [3].

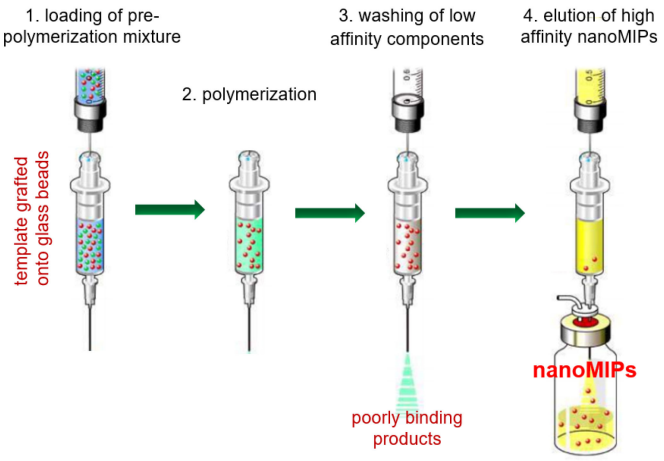

Scheme 1. Representation of the solid-phase synthesis method.

Solid-phase synthesis shows many advantages over traditional solution synthesis techniques. In fact, because template molecules are covalently grafted onto the glass beads, no residual template molecules are present in nanoMIPs, avoiding the bleeding effect that affects many imprinted materials and prevents their practical use [4]. Grafted templates do not need to be soluble in the polymerization solvent, eliminating any issue about solvent-template compatibility [5]. Functionalized glass beads can be cleaned and reused many times, as long as the template does not incur an irreversible denaturation or decomposition during the washing/elution steps [6]. Template reusability has an obvious impact on the costs of synthesis, as it allows the use of expensive molecules, while, in the case of toxic or harmful templates, confinement on the glass surface eliminates any health risks from the residual template during the recover step of the imprinted nanoMIPs [7]. Because of the affinity separation step performed at the end of the polymerization process, nanoMIPs can be easily separated from low affinity products. Thus, they show a more homogenous and significantly higher affinity of the MIPs produced by solution synthesis [3]. Moreover, till nanoMIPs remain attached to the solid support, binding sites are sterically protected, and, thus, post-polymerization modifications are easily achievable [8].

The main feature of the SPSS technique, i.e., the use of a template grafted onto a solid support through a covalent bond, inevitably implies that the imprinting process does not involve the target molecule as is, but, rather, a structural modification of it. To date, most of the target molecules reported in the literature require a simple conjugation reaction between the support and carboxylic, amino, or thiol groups present in the template molecule [2].

In this case, the structural difference between the target and template molecule is minimal, and can be safely ignored when considering the binding affinity and selectivity of the resulting nanoMIPs. On the contrary, in some cases, direct conjugation is not possible or convenient and, analogously to the use of mimic templates in the traditional molecular imprinting technique, a mimic of the target molecule must be considered as template [9]. When the target molecule lacks any functional group suitable for conjugation, a mimic template provided with a suitable functional group must be considered. This is the case for benzoylecgonine and carboxyl-fentanyl, used as mimic templates to prepare nanoMIPs for cocaine and butyrylfentanyl, respectively [10,11]. Moreover, very toxic target molecules can be substituted by less hazardous mimic templates. This is the case for dihydrokainic acid, used as a mimic template to prepare nanoMIPs for domoic acid, a neurotoxin too hazardous to be manipulated [12].

Ochratoxin A (OTA), (Scheme 2, (**1**)), is a mycotoxin produced as a secondary metabolite by several moulds belonging to the *Aspergillus* and *Penicillum* species provided with nephrotoxic, immunosuppressive, teratogenic, and carcinogenic (group 2B) properties [13,14]. OTA is a widespread feed and food contaminant [15,16], and because of this, sample complexity, selective extraction, and clean-up protocols are required before any analytical determination. The conventional sample treatment to remove matrix components is based on the use of

immunoaffinity chromatography, but the use of molecularly imprinted polymers represents an interesting alternative to natural antibodies [17,18].

Concerning nanoMIPs, recently, López-Puertollano et al. reported the use as mimic template of two OTA derivatives named OTAb and OTAe (Scheme 1, (**3**) and (**4**)) to obtain nanoMIPs with good binding properties towards OTA (K_{eq} 2.5 × 10^6 and 2.0 × 10^5 M^{-1}, respectively) [7]. These derivatives were synthetized by adding a spacer arm with six carbon atoms on the phenyl ring in position 7′ (OTAb) and on the carboxyl ring in position 1′ (OTAe) of the OTA molecular skeleton. It is noteworthy that this approach leaves the core structure of the mycotoxin unchanged, and, consequently, requires considerable synthetic efforts [19]. Thus, a mimic template that is structurally simple and cheap to synthesize remains of great interest. It has long been known that the rationally designed mimic N-(4-chloro-1-hydroxy-2-naphthoylamido)-(L)-phenylalanine (CHNA-Phe) (Scheme 1, (**2**)) is able of generating MIPs capable of effectively recognizing OTA. Nevertheless, until now, it has only been used as a mimic template in bulk polymerizations [20–22]. In this work, we wanted to verify if the CHNA-Phe could be a valid mimic template when grafted onto a solid support to be used in the SPPS technique. Thus, nanoMIPs were prepared in conditions strictly analogous to those used by López-Puertollano et al. by using CHNA-Phe grafted onto aminated glass beads, and the binding properties towards the template and towards the OTA proper were measured and compared.

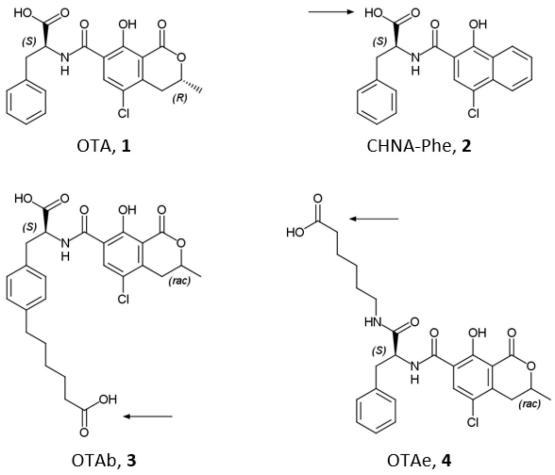

Scheme 2. Molecular structure of Ochratoxin A (**1**), mimic template CHNA-Phe ((**2**), ref. [20]), and mimic templates OTAb and OTAe (**3–4**, refs. [7,19]). Arrows indicate the point of attachment to solid support in SPPS.

2. Materials and Methods

2.1. Materials

Acrylic acid (AA), 2-aminoethylmethacrylate hydrochloride (AEMA), ammonium persulphate (APS), 4-chloro-1-hydroxy-2-naphthoic acid (CHNA), N,N′-diisopropylcarbodiimide (DIC), 1-ethyl-3-(3′-dimethylaminopropyl)carbodiimide hydrochloride (EDAC), ethylenglycole methacrylate phosphate (EGMP), N-hydroxysuccinimide (NHS), N-isopropylacrylamide (NIPAm), N,N′-methylen-bis-acrylamide (BIS), L-phenylalanine (Phe), N-tertbutylacrylamide (TBAm), and N,N,N′,N′-tetramethylethylendiamine (TEMED) were from Sigma-Merck (Milan, Italy).

Solvents and all other chemicals were purchased from Sigma-Merck (Milan, Italy). All the solvents were of HPLC grade, whereas all chemicals were of analytical grade. The water used was ultra-purified in Purelab Prima System from Elga (Marlow, UK). Stock solutions of OTA and CHNA-Phe were prepared by dissolving 25 mg of the substance in 25 mL of water/methanol 1 + 1 (*v*/*v*) and then stored in the dark at −20 °C.

Glass beads (Spheriglass-2429, 70–100 μm average particle size, Potters, UK) were aminated as reported in the literature [23].

2.2. Synthesis of CHNA-Phe

The synthesis was made in accordance to the procedure previously reported in the literature, with minor modifications [22]. In a 100 mL round-bottom flask containing 250 mg (1.13 mmoles) of CHNA dissolved into 25 mL of ice-cold anhydrous, THF were added under stirring 185 µL (1.18 mmoles) of DIC and, after 15 min, 136 mg (1.18 mmoles) of NHS. The mixture was incubated for two hours at 4 °C and then rapidly added drop-by-drop under vigorous stirring in a solution of 560 mg (3.38 mmoles) of L-phenylalanine dissolved in 25 mL of MES buffer (10 mmol L^{-1}, pH 7.4). The reaction mixture was stirred at room temperature overnight, and then evaporated in a rotavapor. The residue was acidified to pH 2 with 0.1 mol L^{-1} aqueous HCl, dispersed under sonication into 25 mL of ethylacetate, and washed three times with 25 mL of acidified water. The organic layer was dried over anhydrous sodium sulphate and evaporated under a stream of air. The raw product obtained was recrystallized twice in absolute ethanol, giving the product as a white powder (324 mg, 78% yield), deemed pure by HPLC-MS with mobile phase MeCN − AcOH, 99 + 1 v/v (eluent A) and water − AcOH, 99 + 1 v/v (eluent B) in A + B gradient from 1 + 9 (1 min) to 9 + 1 (6 min), and then isocratic to 7 min.

Mass spectra: 368 (molecular ion), 324 (M-COOH), 220 (M-$C_6H_5CH_2COOH$), 177 ($C_{10}H_5ClOH$). ^1H NMR ($CDCl_3$, 250 MHz): 11.8 (1H, s, COOH), 8.5 (1H, d, naphtalenic H), 8.2 (1H, d, CONH), 7.8 (4H, d, naphtalenic H), 7.3 (1H, s, naphtalenic H), 6.8 (2H, d, aromatic H), 5.2 (1H, s, aromatic OH), 4.8 (1H, t, CHCOOH).

2.3. Grafting of CHNA-Phe to Glass Spheres

In a 25-mL glass vial containg 22 mg of CHNA-Phe (0.06 mmol) dissolved in 20 mL of anhydrous, THF were added with 140 mg of EDAC (0.6 mmol) and 104 mg of NHS (0.9 mmol). The solution was incubated at 4 °C for 60 min. It was then transferred in 100-mL flask containing 10 g of aminated glass beads in 40 mL of MES buffer (10 mmol L^{-1}, pH 7.4). The suspension was incubated at room temperature overnight, filtered on a 0.22 µm nylon membrane, washed with ultrapure water, rinsed twice with acetone, dried under vacuum at room temperature, and stored in the dark at 4 °C.

2.4. Synthesis of nanoMIPs

The polymerization mixture was prepared in according with the literature [7], with minor modifications and adjusting the dilution of monomers to avoid the formation of unwanted lumps of polymer. A prepolymerization mixture was made in 50 mL of ultrapure water by mixing 1.1 µL of AA (0.016 mmol), 1 mg of AEMA (0.006 mmol), 33.6 mg of EGMP (0.16 mmol), 19 mg of NIPAm (0.17 mmol), 16.5 mg of TBAm (0.13 mmol, previously dissolved in 0.5 mL of ethanol), and 1 mg of BIS (0.0065 mmol). 2 mL of mixture was then added to 25-mL polypropylene SPE cartridge containing 2.5 g of aminated glass beads. The cartridge was purged with nitrogen for 5 min, 15 µL of TEMED and 250 µL of 30 mg mL^{-1} aqueous solution of APS were added, and the polymerization was carried out at room temperature for 60 min. The supernatant was drained by vacuum aspiration, the dry cartridge was cooled to 4 °C, and polymerization by-products and low-affinity nanoMIPs were washed with 3 × 1 mL of ice-cold water. High affinity nanoMIPs were collected by eluting the cartridges with 3 × 1 mL of methanol − acetic acid 99 + 1 (*v/v*). The eluates were evaporated under a stream of nitrogen and stored at 4 °C.

Not-imprinted nanopolymers (nanoNIPs) were prepared by precipitation polymerization in the same experimental conditions in terms of the composition of the polymerization mixture, the quantity of solvent, and the polymerization time, but without the presence of functionalized glass beads. After the polymerization, the slightly opalescent solution was filtered on 0.22 µm nylon membranes to eliminate larger polymers and lyophilized.

2.5. Determination of nanoMIPs Size and Charge

Hydrodynamic particle size and zeta potential were measured with a ZetaView® Nanoparticle Tracking Analyzer PMX-120, (Analytik, Cambridge, UK) using a laser source

at 488 nm. Solid samples of each of the nanoMIPs were dissolved to working dilution with ultrapure water under sonication, the pH was adjusted with HCl 0.1 mol L^{-1}, and about 2 mL of the sample was immediately injected into the Analyzer. The results are the average of three distinct measurements made at 25.5 ± 0.1 °C.

2.6. Atomic Force Microscopy

Borosilicate glass slides, 10 × 10 mm, were washed with 'piranha' solution (98% sulphuric acid + 30% hydrogen peroxide, 3 + 1 *v/v* (caution should be taken because it reacts violently with organic materials) for 10 min, rinsed with ultrapure water, dried under nitrogen, and immersed overnight in a 1% *v*/*v* solution of APTMS in dry toluene. The aminated slides were washed with ethanol and ultrapure water, and then covered with an adequate volume of MES buffer (10 mmol L^{-1}, pH 7.4) containing 1 mg mL^{-1} of NHS-activated nanoMIPs (see Section 2.3), incubated at room temperature overnight, rinsed with ultrapure water, and dried under nitrogen. The Atomic Force Microscopy imaging was performed with a Park System XE–100 microscopes (Park Systems Europe GmbH, Mannheim, Germany) in non-contact mode (scan rate 0.4 Hz) using ACTA-10M cantilevers (Applied Nano Structures, Mountain View, CA, USA).

2.7. Coupling of nanoMIPs to Glass Beads

Covalent coupling of polymer nanoparticles with glass beads was obtained through the formation of an amido link between the acrylic acid residues present on the surface of the nanoparticles and the aminated surface of the glass beads, in according with the literature [23]. In 4-mL glass vials, 2 mg of nanoMIPs were dissolved under sonication in 2 mL of anhydrous THF, and 10 mg of NHS (0.087 mmol) and 14 mg of EDAC (0.058 mmol) were added and then incubated at 4 °C for 60 min. The solution was then transferred in 25-mL flasks containing 2 g of aminated glass beads suspended in 8 mL of MES buffer (10 mmol L^{-1}, pH 7.4), incubated at room temperature overnight, filtered on 0.22 µm nylon membranes, washed with ultrapure water and acetone, dried under vacuum at room temperature, and stored at 4 °C.

2.8. HPLC Method

Reverse phase HPLC analysis was used for OTA and CHNA-Phe quantification. The HPLC apparatus (Merck-Hitachi, Milan, Italy) was a LaChrom Elite system composed of a programmable binary pump L-2130, an auto-sampler L-2200, and a fluorescence detector L-7485, provided with EZChrom Elite software for the instrumental programming, data acquisition, and data processing. The column used was a 100 mm × 4.6 mm Chromolith RP-18 (Merck, Milan, Italy). The mobile phase was acetonitrile/water/acetic acid 40:59:1 (*v/v/v*). Elution was performed in isocratic conditions at a flow rate of 0.5 mL/min. The sample volume injected was 10 µL and the fluorescence wavelength was λ_{ex} = 333/λ_{em} = 460 nm and λ_{ex} = 350/λ_{em} = 416 nm for OTA and CHNA-Phe. In these instrumental conditions, OTA and CHNA-Phe retention times were 3.1 ± 0.1 and 4.6 ± 0.1 min. Standard solutions between 2.5 and 100 ng mL^{-1} were analyzed in triplicate and mean peak areas were plotted against concentration. Calibration plots were drawn by using a weighted linear regression (weight = 1/conc).

2.9. Determination of Binding Properties

To measure binding isotherms, about 40 mg of glass beads supporting nanoMIPs were exactly weighed in 4 mL flat bottom amber glass vials. Then, 1.0 mL of buffered solutions containing increasing amounts of OTA or CHNA-Phe ranging from 2.5 and 100 ng mL^{-1} were added. The vials were incubated overnight at room temperature under continuous agitation on a horizontal rocking table. The solutions were then filtered on 0.22 µm nylon membranes and the free amounts of ligand were measured by HPLC analysis. Each experimental point was assessed as the average of three repeated measures.

Binding parameters were calculated by using SigmaPlot 12 (Systat Software Inc., Richmond, CA, USA). Non-linear least square fitting was applied to the averaged experimental data. Binding isotherm parameters were calculated by using a Langmuir binding isotherm model:

$$B = \frac{B_{max} K_{eq} F}{1 + K_{eq} F}. \quad (1)$$

where B is the ligand bound to the polymer, F is the ligand not bound to the nanoMIPs, K_{eq} is the equilibrium binding constant, and B_{max} is the binding site density. To assure robust results, weighted (1/y) Pearson VII limit minimization was chosen as the minimization method. To avoid being trapped in local minima, which would give incorrect results, minimizations were carried out several times by using different initial guess values for the binding parameters.

Imprinting factor, IF, and Seltivity Index, SI, were calculated as:

$$IF = \frac{K_{eq(MIP)}}{K_{eq(NIP)}} \quad (2)$$

$$SI = \frac{IF_{OTA}}{IF_{CHNA-Phe}} \quad (3)$$

where $K_{eq(MIP)}$ and $K_{eq(NIP)}$ are the equilibrium binding constants of the ligand (CHNA-Phe or OTA) calculated for nanoMIPs and nanoNIPs, respectively.

3. Results and Discussion

To study the ability of the mimic template CHNA-Phe to raise imprinted nanopolymers with molecular recognition properties towards the target molecule OTA, we prepared nanoMIPs by persulfate/TEMED-induced SPPS in water at room temperature. The synthesis, repeated several times, produced batches of nanoMIPs fully soluble in water, resulting in transparent and colorless solutions without any perceivable turbidity. Yields calculated with respect to the amount of monomers in the polymerization mixtures were about 10%. It can be anticipated that the binding properties of the different batches of nanoMIPs were reproducible in terms of equilibrium binding constant, indicating the overall reproducibility of the synthesis approach.

Acrylic acid, ethylenglycole methacrylate phosphate, and 2-aminoethylmethacrylate were used as charged functional monomers, and, thus, nanoMIPs can be seen as charged polyelectrolytes. This is confirmed by ζ potential measurements, where at pH 7 nanoMIPs show a net negative potential of $\zeta = -33.7$ mV, while at pH 3, in more acidic conditions where carboxylic groups are fully protonated but not the phospate, ζ value turns less negative, with $\zeta = -21.4$ mV. The hydrodynamic diameter, d_p, measured by laser nanoparticle tracking at pH 7, shows nanoparticles with an average diameter of 129 ± 66 nm, and with a polydispersity index of 0.26, corresponding to moderately polydispersed nanoparticles.

In a more acidic environment (pH 3 was the instrumental limit of the particle tracker set up), the formation of aggregates larger than 1 μm was indirectly observed, because the nanoparticles count fell by two orders of magnitude from 10^5 to 10^3. About the fraction of nanoparticles remained in solution and the polydispersity index remained essentially constant at 0.26, but the diameter increased markedly to 171 ± 83 nm, doubling the nanoparticles average diameter. These results show that in the solid phase synthesis, the cross-linker structure marginally affects the dimensions of the resulting nanoparticles, which are probably mainly controlled by the formation of dangling long chains of monomers, some or most of which are not cross-linked.

The results obtained by the laser nanoparticle tracking are confirmed by atomic force microscopy performed onto nanoMIPs covalently grafted onto aminosilanized glass slides. The imaging—an example of which is reported in Figure 1—performed on a relatively large area of 10 × 10 μm shows that the glass surface is randomly covered with what seem

to be sparse clusters of nanoparticles with an overall shape rather irregular, apparently composed of several tightly packed globular objects with a slightly wrinkled surface, and with individual diameters comparable to those measured by nanoparticles laser tracking, and therefore compatible with an aggregate of nanoparticles.

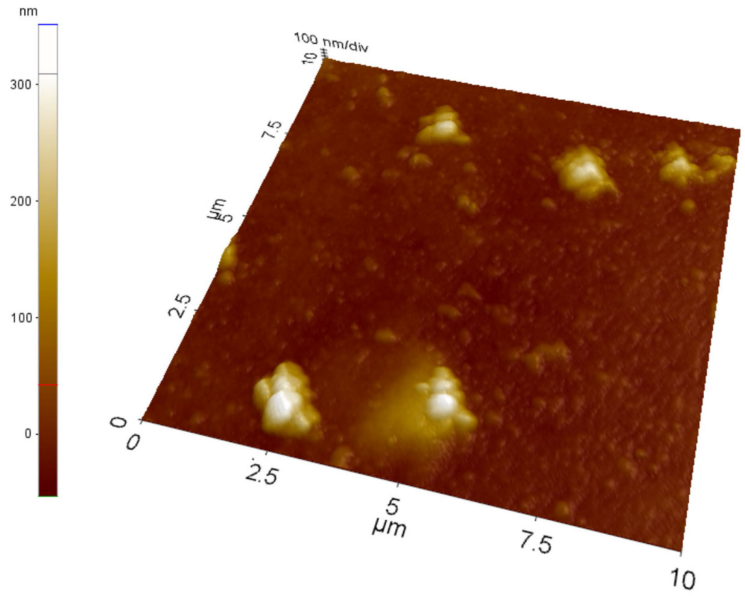

Figure 1. AFM of a glass slide covalently grafted at pH 7.4 with CHNA-Phe-imprinted nanoMIPs.

The binding parameters obtained from binding isotherm measured in phosphate buffers at a different pH between 4 and 8 for CHNA-Phe and OTA (Figure 2) are reported in Table 1. NanoMIPs prepared by SPPS strongly bind the mimic template CHNA-Phe and, likewise, the target molecule OTA with equilibrium binding constants (K_{eq}) in the range of 10^6 L mol^{-1}, showing at pH of 6–7 affinity values comparable to those reported by López-Puertollano et al. using OTAb and OTAe as mimic templates [7]. The statistical comparison (two-way *t*-test: = 0.05, n = 10, t < 2.101) between the equilibrium binding constants for CHNA-Phe and OTA measured onto the nanoMIPs show that the values are indistinguishable from each other, therefore demonstrating that CHNA-Phe is a very effective mimic template in eliciting imprinting binding sites capable of recognizing OTA.

Table 1. Equilibrium binding constants (±1 standard error unit) measured for CHNA-Phe and OTA on CHNA-Phe-imprinted nanoMIPs and nonimprinted nanoMIPs.

	nanoMIPs		**nanoNIPs**	
pH Buffer	**CHNA-Phe (10^6 L mol^{-1})**	**OTA (10^6 L mol^{-1})**	**CHNA-Phe (10^6 L mol^{-1})**	**OTA (10^6 L mol^{-1})**
4	1.52 ± 0.98	1.11 ± 0.62	0.54 ± 0.30	0.60 ± 0.53
5	3.67 ± 0.63	3.71 ± 1.00	1.61 ± 0.43	1.92 ± 0.71
6	8.34 ± 1.82	7.80 ± 1.88	1.91 ± 0.33	1.88 ± 0.87
7	6.58 ± 0.99	5.58 ± 0.55	1.33 ± 0.22	1.57 ± 0.41
8	1.46 ± 0.35	1.36 ± 1.04	0.88 ± 0.66	1.32 ± 0.34

It can be seen that the magnitude of molecular recognition depends on the buffer pH, and it can be related to the ionization state of ligands and functional monomers in the binding site. Concerning the ligands, OTA has two substituents that exhibit acid-base properties: the phenolic hydroxyl at position 8 on the dihydroisocoumarinic substructure, with pK 7.0–7.3, and the carboxyl at position 2′ on the phenylalanine substructure, with pK 4.2–4.4 [24]. Regarding CHNA-Phe, no experimental values are available, but in silico calculations indicate values very similar to those of the OTA [25]. Concerning the

functional monomers, it is necessary to underline how the paper of López-Puertollano et al. has highlighted how AEMA, due to its ability to interact with both the ionizable substituents of the ligands, is presumably the key functional monomer in determining the molecular recognition properties of nanoMIPs [14]. In the light of this observation, it is therefore possible to easily explain how the pH influences the molecular recognition. At pH 4, the carboxyl at position 2′ is predominantly protonated, and therefore unable to interact with the amino function of the AEMA, which is protonated and positively charged. From pH 5 onwards, however, the carboxyl becomes deprotonated, and therefore capable of interacting through an ionic bond with the amino function, increasing the magnitude of the molecular recognition. At pH 8, the amine also deprotonates [26], thus losing, again, the ability to give an ionic interaction with the carboxylate ion. Concerning the phenolic substituent, it is possible that when it is in a protonated neutral form, it is capable of interacting with the phosphate group of the functional monomer EGMP through the formation of a cyclic hydrogen bond reported for organic phosphates in the literature [27], but this structure would be missing at pH 8 when the phenolic function deprotonates, weakening the magnitude of molecular recognition.

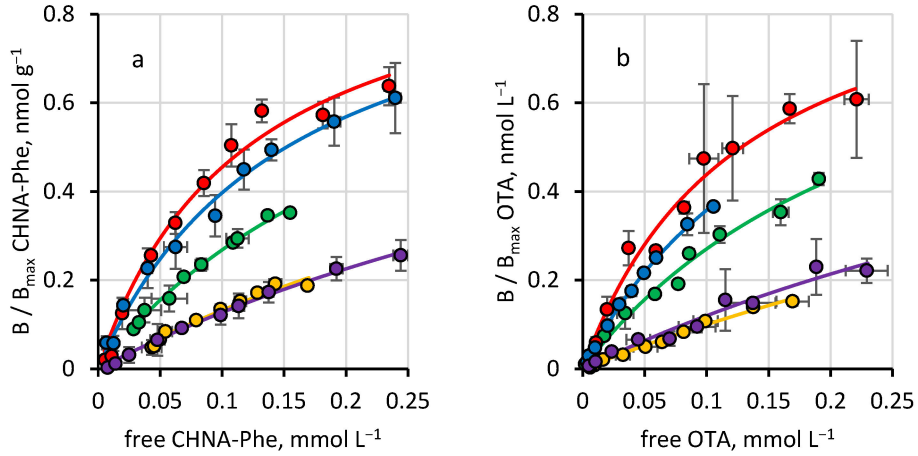

Figure 2. Binding isotherm for CHNA-Phe (**a**) and OTA (**b**) measured on CHNA-Phe-imprinted nanoMIPs. Yellow: pH 4; green: pH 5; red: pH 6; blue: pH 7; violet: pH 8.

The presence of nonspecific binding was investigated by measuring the binding isotherms in aqueous buffers onto nanoNIPs (Figure 3) and calculating the equilibrium binding constants of CHNA-Phe and OTA. Because it is reasonable that the binding between ligands and nanoNIPs is exclusively due to interactions not dependent on molecular recognition effects, an estimate of the magnitude of the molecular imprinting effect can thus be easily evaluated considering the imprinting factor (IF) for CHNA-Phe and OTA reported in Table 2. The statistical comparison (two-way *t*-test: = 0.05, $n = 10$, $t < 2.101$) between IFs calculated for CHNA-Phe and OTA show that the values are indistinguishable from each other—except for the values at pH 7, where IF for CHNA-Phe is significantly higher—again confirming that CHNA-Phe is a very effective mimic template in eliciting imprinting binding sites capable of recognizing OTA. However, a statistical evaluation (one-way *t*-test: = 0.05, $n = 10$, $t < 2.101$) of how far the IF values actually deviate from unity (no imprinting effect at all) shows clearly that pH exerts an influence on the molecular recognition. In fact, values of IF calculated for the binding in acid (pH = 4) or basic (pH = 8) buffers do not differ significantly from the unit, indicating that in such pH, the molecular recognition effect is only apparent.

From IF values, it is also possible to calculate the selectivity index (SI), a parameter allowing us to directly compare the binding of different ligands to an MIP, taking care of non-specific binding [28] but considering a mimic imprinting, and it can also be useful to compare the binding of the target ligand relative to that of the mimic template. In this case, values of SI greater than unity indicate that the latter is recognized less than the

former and vice versa. As reported in Figure 4, the SI of CHNA-Phe nanoMIPs towards OTA allows us to achieve a more precise view of the molecular recognition of the OTA by nanoMIPs. In fact, SI values for OTA are relatively high but systematically less than unity. This confirms again that OTA is slightly less recognized than the mimic template, showing, at the same time, that the substantial identity of the equilibrium binding constants reported in Table 1 is due to the presence of a small but not negligible non-specific contribution that is independent of the buffer pH.

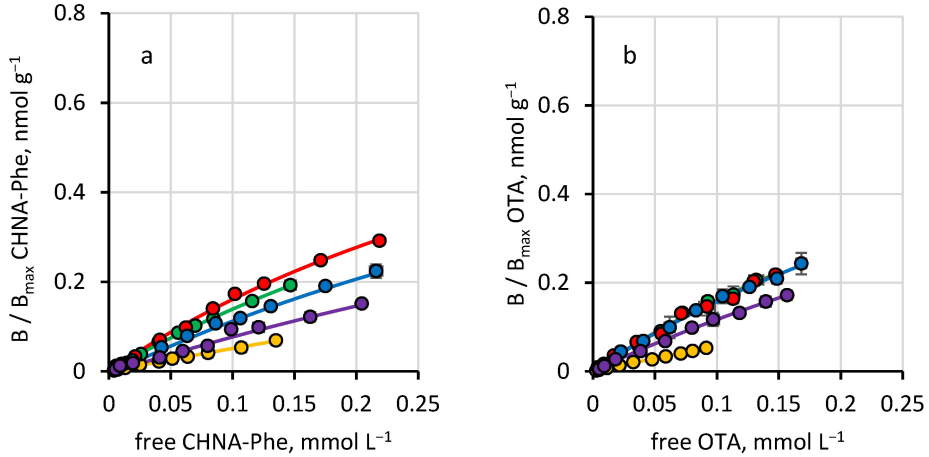

Figure 3. Binding isotherm for CHNA-Phe (**a**) and OTA (**b**) measured on nanoNIPs. Yellow: pH 4; green: pH 5; red: pH 6; blue: pH 7; violet: pH 8.

Table 2. Imprinting factors (±1 standard error unit) calculated for CHNA-Phe and OTA.

pH Buffer	CHNA-Phe	OTA
4	2.83 ± 2.41	1.85 ± 1.93
5	2.28 ± 0.72	1.94 ± 0.88
6	4.37 ± 1.22	4.14 ± 2.17
7	4.95 ± 1.11	3.55 ± 0.26
8	1.66 ± 1.31	1.03 ± 0.83

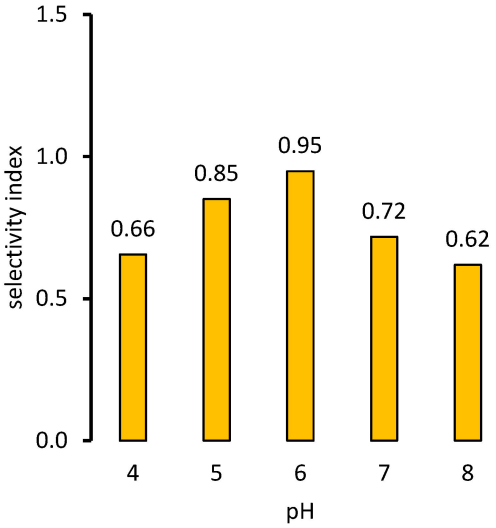

Figure 4. Selectivity index of CHNA-Phe nanoMIPs towards OTA.

4. Conclusions

Overall, these results confirm that the SPPS approach is indeed more effective than classical methods in preparing OTA binding MIPs, as molecular recognition can be elicited

in an aqueous environment, generating highly affine and selective binding sites. The use of CHNA-Phe as a template demonstrates that it is possible and convenient to use, as mimic templates, molecules whose three-dimensional structure is to some extent different from the target molecule without a substantial loss of selectivity or binding affinity.

Author Contributions: Conceptualization, C.B.; methodology, T.S.; formal analysis, F.D.N.; investigation, T.S. and V.T.; writing—original draft preparation, T.S. and M.C.; writing—review and editing, S.C.; supervision, L.A. and C.B. All authors have read and agreed to the published version of the manuscript.

Funding: Authors acknowledge support from the Project CH4.0 under the MUR program "Dipartimenti di Eccellenza 2023-2027" (CUP: D13C22003520001).

Data Availability Statement: The data presented in this study are available on request from the corresponding author.

Conflicts of Interest: The authors declare no conflict of interest.

References

1. Wackerlig, J.; Schirhagl, R. Applications of molecularly imprinted polymer nanoparticles and their advances toward industrial use: A review. *Anal. Chem.* **2016**, *88*, 250–261. [CrossRef] [PubMed]
2. Cowen, T.; Stefanucci, E.; Piletska, E.; Marrazza, G.; Canfarotta, F.; Piletsky, S.A. Synthetic mechanism of molecular imprinting at the solid phase. *Macromolecules* **2020**, *53*, 1435–1442. [CrossRef]
3. Canfarotta, F.; Poma, A.; Guerreiro, A.; Piletsky, S. Solid-phase synthesis of molecularly imprinted nanoparticles. *Nat. Protoc.* **2016**, *11*, 443–455. [CrossRef] [PubMed]
4. Lorenzo, R.A.; Carro, A.M.; Alvarez-Lorenzo, C.; Concheiro, A. To remove or not to remove? The challenge of extracting the template to make the cavities available in molecularly imprinted polymers (MIPs). *Int. J. Mol. Sci.* **2011**, *12*, 4327–4347. [CrossRef]
5. Smolinska-Kempisty, K.; Guerreiro, A.; Canfarotta, F.; Cáceres, C.; Whitcombe, M.J.; Piletsky, S.A. Comparison of the performance of molecularly imprinted polymer nanoparticles for small molecule targets and antibodies in the ELISA format. *Sci. Rep.* **2016**, *6*, 37638. [CrossRef]
6. Poma, A.; Guerreiro, A.; Caygill, S.; Moczko, E.; Piletsky, S. Automatic reactor for solid-phase synthesis of molecularly imprinted polymeric nanoparticles (MIP NPs) in water. *RSC Adv.* **2014**, *4*, 4203–4206. [CrossRef]
7. López-Puertollano, D.; Cowen, T.; García-Cruz, A.; Piletska, E.; Abad-Somovilla, A.; Abad-Fuentes, A.; Piletsky, S. Study of epitope imprinting for small templates: Preparation of nanoMIPs for Ochratoxin A. *ChemNanoMat* **2019**, *5*, 651–657. [CrossRef]
8. Moczko, E.; Guerreiro, A.; Piletska, E.; Piletsky, S. PEG-stabilized core−shell surface-imprinted nanoparticles. *Langmuir* **2013**, *29*, 9891–9896. [CrossRef]
9. Fresco-Cala, B.; Mizaikoff, B. Surrogate imprinting strategies: Molecular imprints via fragments and dummies. *ACS Appl. Polym. Mater.* **2020**, *2*, 3714–3741. [CrossRef]
10. Smolinska-Kempisty, K.; Sheej Ahmad, O.; Guerreiro, A.; Karim, K.; Piletska, E.; Piletsky, S. New potentiometric sensor based on molecularly imprinted nanoparticles for cocaine detection. *Biosens. Bioelectron.* **2017**, *96*, 49–54. [CrossRef]
11. Liu, L.L.; Grillo, F.; Canfarotta, F.; Whitcombe, M.; Morgan, S.P.; Piletsky, S.; Correia, R.; He, C.Y.; Norris, A.; Korposh, S. Carboxyl-fentanyl detection using optical fibre grating-based sensors functionalised with molecularly imprinted nanoparticles. *Biosens. Bioelectron.* **2021**, *177*, 113002. [CrossRef]
12. Quezada, C.; Vera, M.; Barraza, L.F.; García, Y.; Pereira, E.D. Molecularly imprinted nanoparticle-based assay (MINA): Potential application for the detection of the neurotoxin domoic acid. *Anal. Chim. Acta* **2021**, *1181*, 338887. [CrossRef]
13. Pfohl-Leszkowicz, A.; Mandeville, R.A. Ochratoxin A: An overview on toxicity and carcinogenicity in animals and humans. *Mol. Nutr. Food Res.* **2007**, *51*, 61–99. [CrossRef]
14. Heussner, A.H.; Bingle, L.E.H. Comparative Ochratoxin toxicity: A review of the available data. *Toxins* **2015**, *7*, 4253–4282. [CrossRef]
15. Duarte, S.C.; Peña, A.; Lino, C.M. A review on Ochratoxin A occurrence and effects of processing of cereal and cereal derived food products. *Food Microbiol.* **2010**, *27*, 187–198. [CrossRef]
16. Duarte, S.C.; Lino, C.M.; Peña, A. Ochratoxin A in feed of food-producing animals: An undesirable mycotoxin with health and performance effects. *Vet. Microbiol.* **2011**, *154*, 1–13. [CrossRef]
17. Yu, J.C.C.; Lai, E.P.C. Molecularly imprinted polymers for ochratoxin A extraction and analysis. *Toxins* **2010**, *2*, 1536–1553. [CrossRef]
18. Pichon, V.; Combès, A. Selective tools for the solid-phase extraction of Ochratoxin A from various complex samples: Immunosorbents, oligosorbents, and molecularly imprinted polymers. *Anal. Bioanal. Chem.* **2016**, *408*, 6983–6999. [CrossRef]
19. López-Puertollano, D.; Mercader, J.V.; Agulló, C.; Abad-Somovilla, A.; Abad-Fuentes, A. Novel haptens and monoclonal antibodies with subnanomolar affinity for a classical analytical target, Ochratoxin A. *Sci. Rep.* **2018**, *8*, 9761. [CrossRef]
20. Baggiani, C.; Giraudi, G.; Vanni, A. A molecular imprinted polymer with recognition properties towards the carcinogenic mycotoxin Ochratoxin A. *Bioseparation* **2001**, *10*, 389–394. [CrossRef]

21. Jodlbauer, J.; Maier, M.M.; Lindner, W. Towards Ochratoxin A selective molecularly imprinted polymers for solid-phase extraction. *J. Chromatogr. A* **2002**, *945*, 45–63. [CrossRef] [PubMed]
22. Baggiani, C.; Biagioli, F.; Anfossi, L.; Giovannoli, C.; Passini, C.; Giraudi, G. Effect of the mimic structure on the molecular recognition properties of molecularly imprinted polymers for Ochratoxin A prepared by a fragmental approach. *React. Funct. Polym.* **2013**, *73*, 833–837. [CrossRef]
23. Cavalera, S.; Chiarello, M.; Di Nardo, F.; Anfossi, L.; Baggiani, C. Effect of experimental conditions on the binding abilities of ciprofloxacin-imprinted nanoparticles prepared by solid-phase synthesis. *React. Funct. Polym.* **2021**, *163*, 104893. [CrossRef]
24. Perry, J.L.; Christensen, T.; Goldsmith, M.R.; Toone, E.J.; Beratan, D.N.; Simon, J.D. Binding of Ochratoxin A to human serum albumin stabilized by a protein-ligand ion pair. *J. Phys. Chem. B* **2003**, *107*, 7884–7888. [CrossRef]
25. MarvinSketch 20.4. Available online: http://www.chemaxon.com (accessed on 8 March 2023).
26. Thompson, K.L.; Read, E.S.; Armes, S.P. Chemical degradation of poly(2-aminoethyl methacrylate). *Polym. Degrad. Stab.* **2008**, *93*, 1460–1466. [CrossRef]
27. Cuypers, R.; Sudhölter, E.J.R.; Zuilhof, H. Hydrogen bonding in phosphine oxide/phosphate–phenol complexes. *ChemPhysChem* **2010**, *11*, 2230–2240. [CrossRef]
28. Cheong, S.H.; McNiven, S.; Rachkov, A.; Levi, R.; Yano, K.; Karube, I. Testosterone receptor binding mimic constructed using molecular imprinting. *Macromolecules* **1997**, *30*, 1317–1322. [CrossRef]